J Dent Sci 2010;5(3):156–165

ELSEVIER

ORIGINAL ARTICLE

Effects of implant threads on the contact area and stress distribution of marginal bone

Chia-Ching Lee,[1,2] *Shang-Chih Lin,*[1,2] *Ming-Jen Kang,*[1,2] *Shu-Wei Wu,*[1,2] *Ping-Yuen Fu*[3,4*]

[1]Institute of Biomedical Engineering, National Central University, Taoyuan, Taiwan
[2]Department of Mechanical Engineering, National Central University, Taoyuan, Taiwan
[3]School of Dentistry, College of Oral Medicine, Taipei Medical University, Taipei, Taiwan
[4]Goldman School of Dental Medicine, Center for Implantology, Boston University, Boston, MA, USA

Received: May 13, 2010
Accepted: Aug 27, 2010

KEY WORDS:
bone stress;
contact area;
dental implant;
marginal bone loss;
thread

Background/purpose: Stable osseointegration between implant threads and the surrounding marginal bone provides the mechanical base of an implant for daily chewing activity. The contact area of implant-bone interfaces and the concentrated stresses on the marginal bones are principal concerns of implant designers. The purpose of this study was to investigate the effects of thread shape and taper on the initial stability of the implant-bone structure.
Materials and methods: The thread design was parameterized by shape and taper. Thread shapes included symmetrical, square, and buttressed. Thread tapers were divided into cylindrical and conical profiles. Nine variations of the thread design were developed to numerically evaluate their geometric and mechanical effects on the marginal bone.
Results: Among the three thread shapes with the same pitch, the contact area of the square thread was the highest. Among all implant models, it was found that the site with the greatest stress in the surrounding jaw bone was consistently concentrated at the root radii of the first thread. The maximal stress of the square thread was the least. For the same thread shape and taper, a finer pitch resulted in a remarkable increase in the contact area and a decrease in the peak stress. The contact areas and peak stresses of the conical and cylindrical implants were nearly equal.
Conclusion: Taking wall thickness and stress concentrations into consideration, the square thread with a 0.60-mm pitch possessed the optimal contact area and stress values compared to the others.

Introduction

To rehabilitate missing dentition, treatment with fixed dentures often requires reshaping of the configuration of the neighboring healthy teeth. In addition, the remaining teeth might not provide sufficient support and retention for daily chewing function with removable dentures. Consequently, dental implants have gradually become one of the main treatment modalities to rehabilitate missing teeth.[1–5] The principal function of implants is to stably support the prosthesis after osseointegration with the jaw bone. Two types of interfacial fixation are necessary for successful stabilization of the

*Corresponding author. College of Dental Science, Taipei Medical University, 250, Wu-Hsing Street, Taipei 11042, Taiwan.
E-mail: sonnyfu2004@yahoo.com

implant-bone structure. The first is mechanical fixation by the implant threads. This is the main contributing factor to the initial stability of the implant itself. However, for long-term stabilization, the second is biological fixation, which is necessary for further osseointegration of the inserted surfaces of the implant by the surrounding bone. Historically, determining how to enhance the efficiency of both fixation types is a well-known active topic of implant research.[6,7]

Osseointegration is reported to be affected by many factors, including the implant design, surface treatment, bone quality, surgical technique, postoperative care, and so on.[8–10] Among these, the thread design of an implant is one of the dominant factors.[11] Previous studies reported that the total contact area between the implant and bone plays a significant role in the osseointegration strength of implant-bone interfaces.[10,11] In addition, the design of the implant threads directly affects the stress distribution and marginal bone resorption.[12,13]

Theoretically, the contact area and stress distribution of bone-implant interfaces are closely related to the values of those parameters. Among them, the pitch and two flank angles dominantly affect the pull-out and push-in strengths of bone chips sandwiched by the implant threads.[14,15] Additionally, the fatigue strength of the implant threads is affected by the height, pitch, and especially the two root radii of the implant threads.[16,17] In the literature, many numerical and clinical reports revealed that the first thread is the most stressed site, and thus the initial microfracture and eventually immature osseointegration occur at this site.[18] There are various types of dental implants for clinical use, and designs of the thread shape and taper differ greatly among them.

In this study, the geometric and mechanical effects of thread design on the marginal bone were evaluated. First, nine implant variations of thread shapes and tapers were developed to compare the values of the total contact area among them. Subsequently, a finite-element method was used to investigate the effects of thread design on the stress distribution of the marginal bone, especially at the first thread.

Materials and methods

Implant and bone models

In this study, the thread design was divided into two categories: thread shape and taper. Generally, the thread shape is defined by seven constitutive parameters (Fig. 1). The conical and cylindrical profiles of the threaded portion are two common

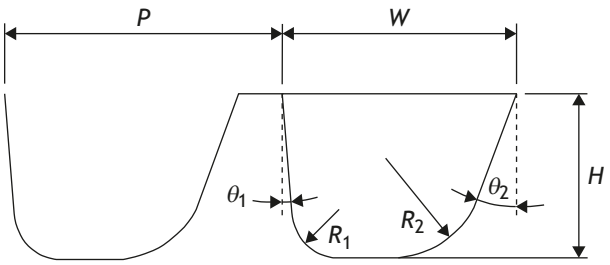

Fig. 1 Constitutive parameters of typical implant threads including pitch (*P*), width (*W*), height (*H*), flank angles (θ_1 and θ_2), and root radii (R_1 and R_2).

types of thread taper (Fig. 2A). In this study, three types of thread shape were investigated: symmetrical, square, and buttressed (Figs. 2A and 2B). The thread height and width were, respectively, 0.35 mm and 0.50 mm for all types of thread shape. The commonly used thread for commercially available implants has a 0.60-mm pitch. However, the 0.60-mm pitch and 0.50-mm width cause the square thread to have a very thin wall thickness (=0.10 mm). Hence, especially for square threads, threads with a 0.80-mm pitch were also used in this study (Fig. 2B). The 0.6-mm pitch of the implants was further divided into cylindrical and conical types according to the thread taper along the implant axis (Fig. 2A). Each inner and outer diameter of the cylindrical type was uniform along the implant axis. For the conical implant, the thread depth was constant and the outer diameter gradually decreased toward the implant tip, with a tapering angle of 2.0°. Consequently, there were nine variations (3 thread forms $\times$1 conical thread $\times$1 thread pitch +3 thread forms $\times$1 cylindrical thread $\times$2 thread pitches) in this study. For the nine implant models, the outer diameter at the screw hub and the length of the threaded portion were 3.80 mm and 10.0 mm, respectively. The current study assumed that the cutting flutes at the implant tip and the interconnective mechanism at the implant/abutment interfaces had minor effects on the stress distribution at the first thread. Hence, the cutting flutes and interconnective mechanism were not evaluated in this study.

The implants with the aforementioned nine variations were inserted into the bone block which consisted of cylindrically shaped cortical and cancellous bones (Fig. 3A). The outer diameter and depth of the cortical and cancellous bones were, respectively, ϕ 10$\times$2 mm and ϕ 10$\times$10 mm. The collar of the implant made contact with the cortical block. The threaded portion of the inserted implant was fully within the cancellous bone. In this study, the three-dimensional models of the implant and bone block were created by SolidWorks 2008 software (SolidWorks Corp., Concord, MA, USA).

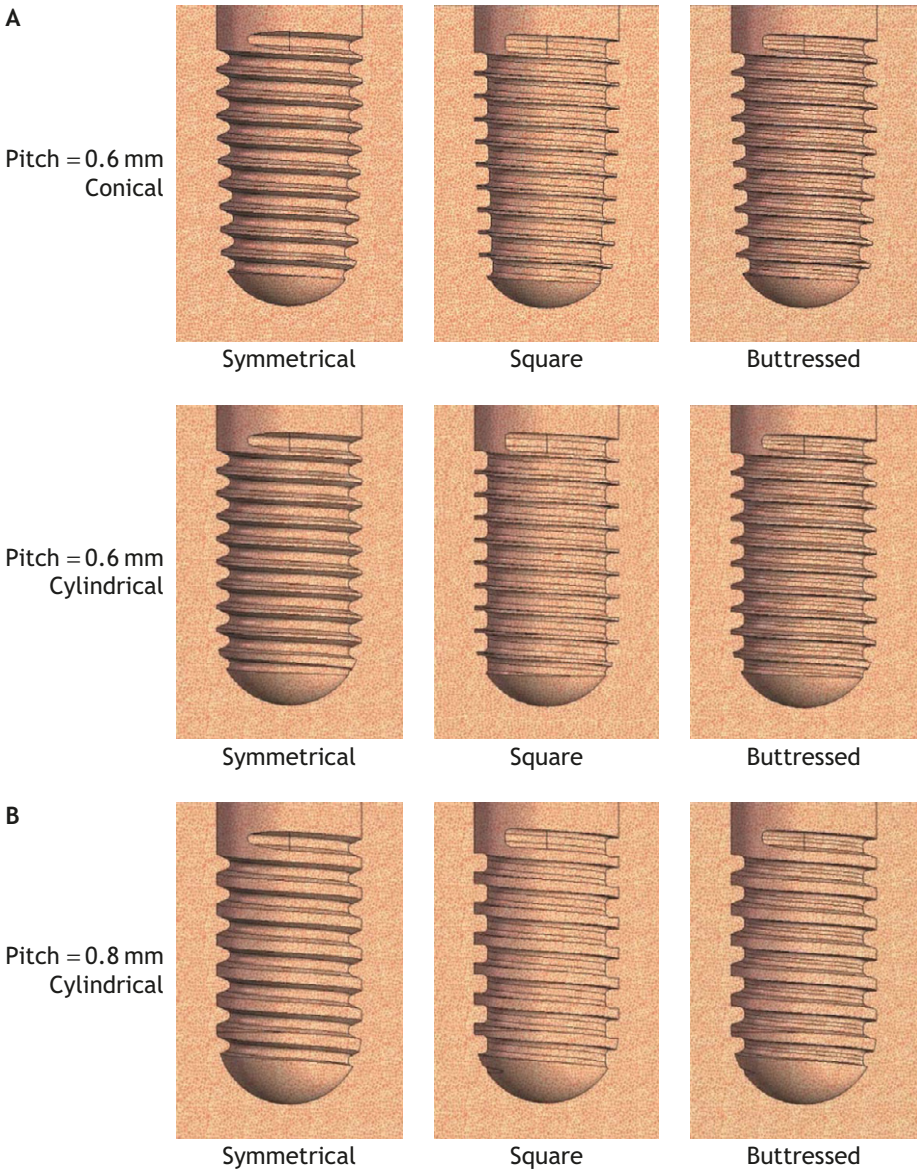

Fig. 2 (A) Two types of thread taper along the implant axis: conical and cylindrical. Three types of thread shape were studied in the finite-element analyses: symmetrical thread, $\theta_1=\theta_2=30°$ and $R_1=R_2=0.15$ mm; square thread, $\theta_1=\theta_2=0°$ and $R_1=R_2=0.15$ mm; and buttressed thread, $\theta_1=5°$, $\theta_2=20°$, and $R_1=R_2=0.15$ mm. The thread width of all thread shapes was consistently 0.50 mm. There was one pitch of 0.6 mm for each thread shape. (B) As above, the three types of thread shape were the same. There was one pitch of 0.8 mm for each thread shape.

Finite-element analyses

The finite-element model established in this study included the implant and two bone blocks (Fig. 3A). The material properties of all three materials were assumed to be isotropic and linearly elastic.[19,20] The implant was made of Ti-6Al-4V, for which Young's modulus and the Poisson ratio were, respectively, 110 GPa and 0.32. Young's moduli of the cortical and cancellous bones were, respectively, 14.8 and 3.0 GPa, while the Poisson ratios of both were identical at 0.3.[21–23] In this study, the maximum von Mises stress of each component was compared with its yield strength to validate the material assumption of linear elasticity. The current study attempted to investigate the effects of thread shape and taper on the initial stability of the implant-bone structure. For the initial stability, the interfaces between the implant and bone blocks were assumed to be not fully osseointegrated. The load-transfer property of the implant-bone interface was simulated to behave as a node-to-node contact element without friction. Nodes at the bottom of the cylindrical bone block were assumed to be fully fixed (Fig. 3A). As shown in Fig. 3A, the top of the implant was subjected to an axial load of 100 N and an oblique load of 100 N at a 15° incline to the implant axis.[12,24]

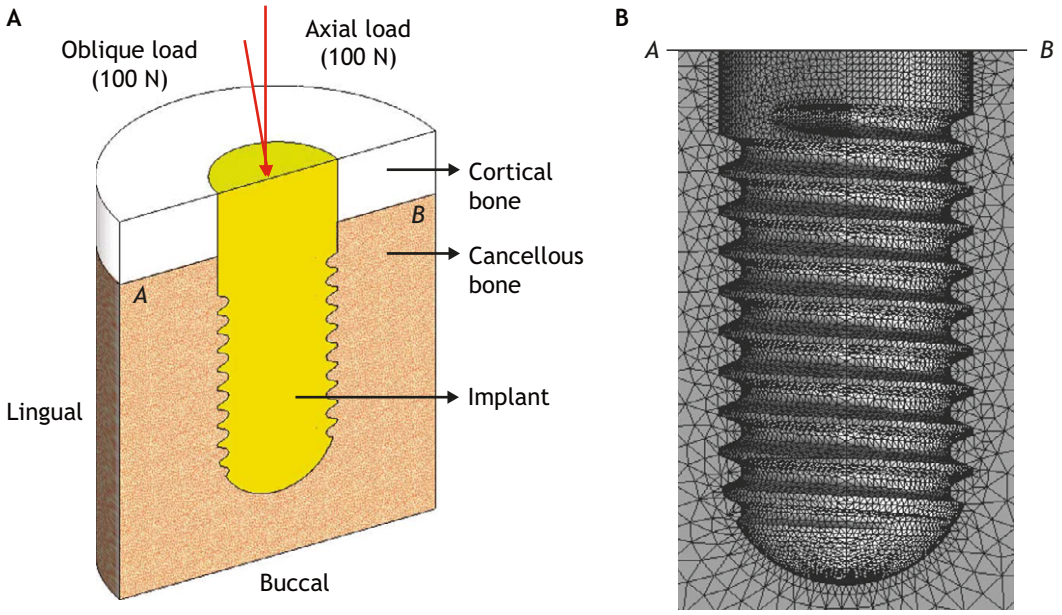

Fig. 3 (A) The finite-element model used in this study. The chewing forces were directly applied to the superior surface of the implant. (B) The vertically sectioned model illustrates the mesh strategy of local control of the element size, especially at highly stressed sites.

To determine the accuracy of the calculated stresses, the local controls for the higher mesh density were given at the threaded portion of the implant-bone interface, especially at the first mandible thread (Fig. 3B). Both root radii of the thread were meshed with a 0.10-mm element size, and the value of the other threaded surfaces was about 0.20 mm. However, the 0.05-mm element size at the first thread was, on average, 10-fold denser than the other sites of the implant and bone models. In this study, the curved boundary of the 10-node tetrahedral solid element was designed as the meshing strategy. There were no sharp discontinuities which could induce an unrealistically high stress concentration. Using the aspect ratio and Jacobian checks, all elements were within acceptable distortion limits, thus maximizing the accuracy of the results. On average, numbers of elements and nodes were 528,000 and 693,000, respectively, for the nine models. The meshing, analysis, and post-processing of the nine models used the COSMOSWorks Ed. 2008 software (SolidWorks Corp.).

Comparative indices

Four indices were used to explain and discuss the results of this finite-element study. The first index was the total contact area between the threaded portion of the implant and the smooth portion of the surrounding bone (Fig. 3B). The value of the total contact area was directly obtained using SolidWorks commands. The second index was the distribution of the von Mises stress for each thread along the implant axis. This index was used to verify whether the most-stressed site was at the first thread, as reported in the literature. If this was consistent with other literature reports, the third index was a comparison of the maximum stress at the first thread of the nine implant models. The fourth index further compared differences in the statistical distributions of nodal stresses of the nine implant models within that high-stress-concentrated site. The average stresses of the nodes within the definite area of the first thread were calculated and compared to the maximum stress, which is commonly chosen as a comparison index in the literature. This index can provide information regarding the effect of the thread shape and taper on the stress of the first thread.

Results

Contact area

Fig. 4 shows values of the total contact area for the nine implant models. For the symmetrical, square, and buttressed threads, contact areas of the conical implant were, respectively, 1.5%, 0.7%, and 0.7% less than that of the corresponding cylindrical one. For the cylindrical implant, contact areas of the symmetrical, square, and buttressed threads with the 0.60-mm pitch were, respectively, 7.3%, 9.0%, and 7.8% higher than those with the 0.80-mm pitch. Among both thread pitches, the contact area of the square thread was the highest, followed by the buttressed one, with the symmetrical one the smallest.

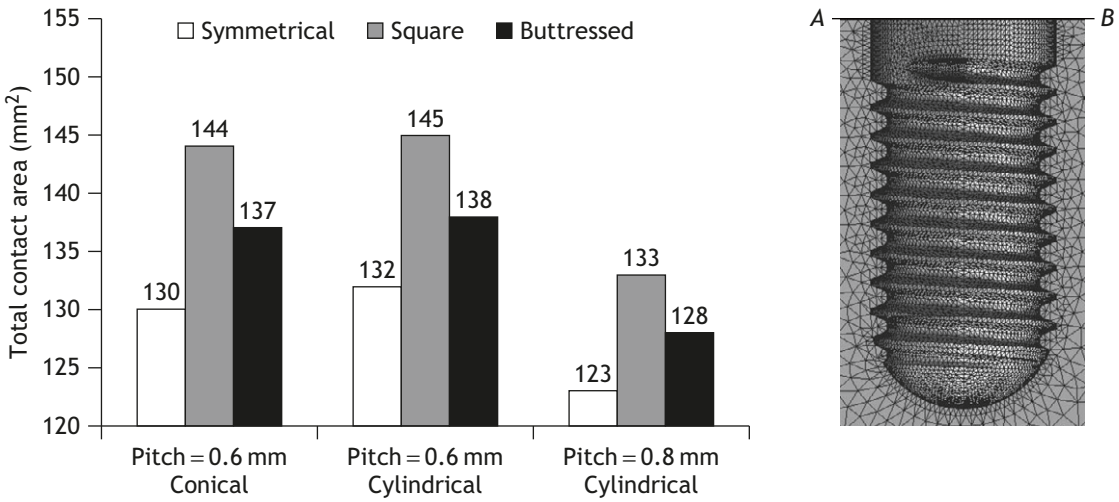

Fig. 4 Values of the total contact area for the nine implants. The contact area was defined as the surface area between the implant-bone interface, ranging from the implant tip to line *AB*.

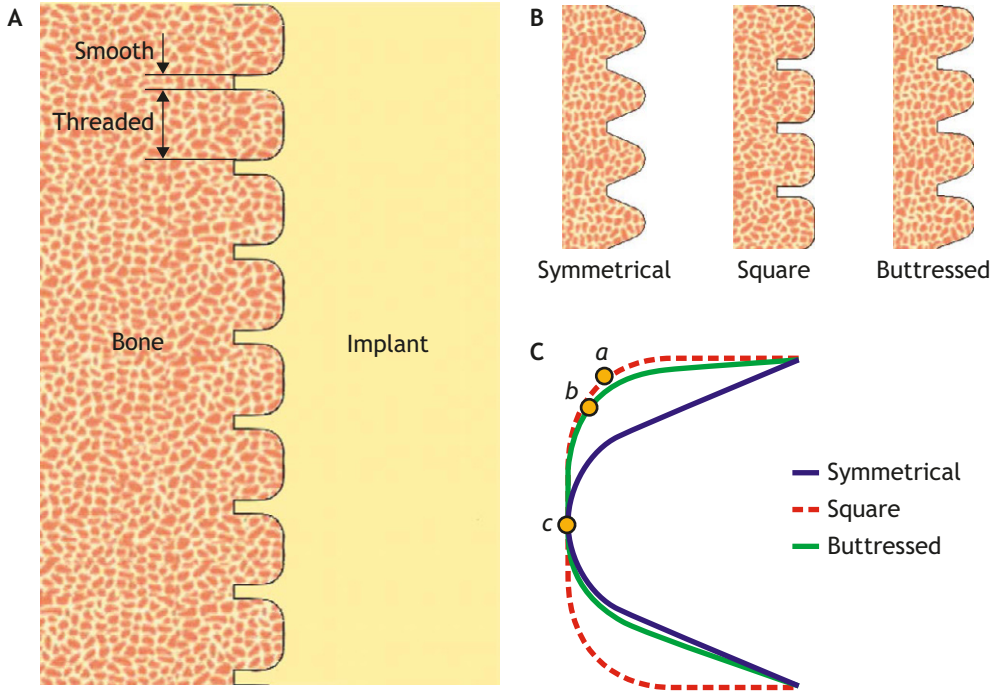

Fig. 5 (A) After the pilot drilling, the mandible threads were formed by subsequent extrusion for insertion of the implant. The diagram shows the serial mandible threads along the implant axis. The smooth and threaded portions of a single implant thread are indicated. (B) Mandible threads for the symmetrical, square, and buttressed threads. (C) Three thread profiles were calculated and compared. Stress-concentration sites for the three thread shapes are indicated by the points *a* (square), *b* (buttressed), and *c* (symmetrical).

The contact area of the conical square thread with a 0.6-mm pitch was 10.8% and 5.1% higher than those of the corresponding symmetrical and buttressed ones. For the 0.60-mm pitch, the contact area of the cylindrical square thread was 9.8% and 5.1% higher than those of the symmetrical and buttressed ones. Comparatively, respective differences in areas of the symmetrical and buttressed threads compared to the square thread were 8.1% and 4.0% for the 0.80-mm pitch. There were 10 and seven threads for the 0.60-mm and 0.80-mm pitches, respectively (Figs. 2A and 2B).

Assuming the bone to be a continuous material, Fig. 5A shows a schematic diagram of the implant-bone interfaces. During implant insertion, the bone block was deformed to accommodate the thread profile around the insertion hole (Fig. 5B). For the symmetrical, square, and buttressed threads, the

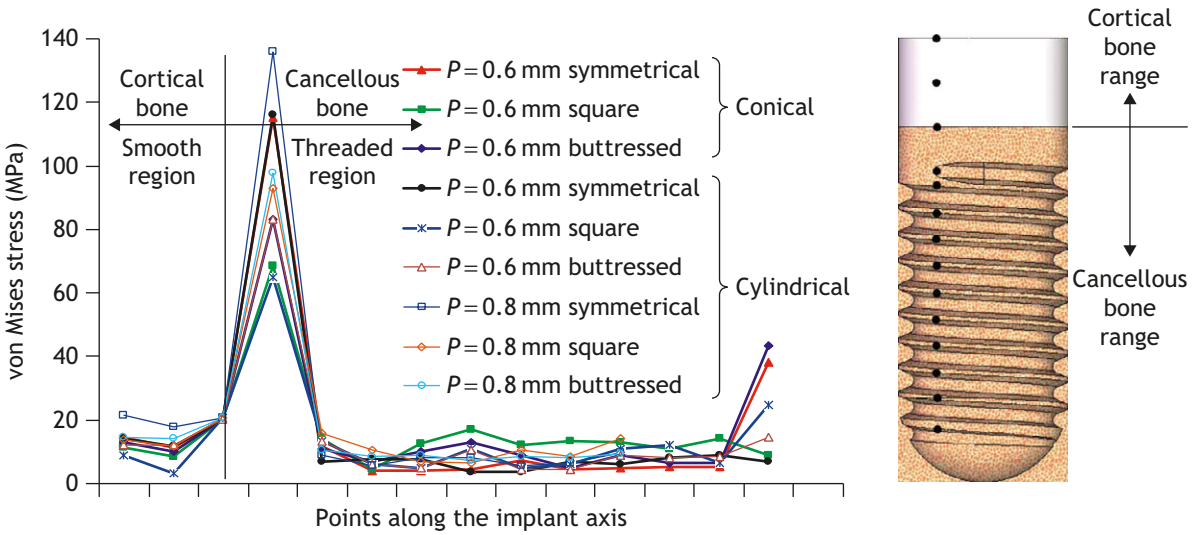

Fig. 6 For the nine implant designs, the von Mises stress of each mandible thread is shown by the 14 points along the implant axis. The first three points were set in the smooth region, while the other points were in the threaded region. *P*=pitch.

cross-sectional areas of the single mandible thread were 0.12 mm^2, 0.17 mm^2, and 0.14 mm^2, respectively. Area values of the single square thread were 41.7% and 21.4% higher than those of the symmetrical and buttressed threads. This study assumed that the mechanical strength and stress value of a thread were closely related to its cross-sectional area. Fig. 5C shows the circumferential length of a single thread projected onto the sagittal plane. Circumferential lengths of the single symmetrical, square, and buttressed threads were 0.91 mm, 1.07 mm, and 0.99 mm, respectively. The circumferential length of the square thread was again the highest, and was 17.6% and 8.1% higher than those of the symmetrical and buttressed threads, respectively. For the three thread shapes, the most stressed sites consistently occurred at the thread root (Fig. 5C). This demonstrates that the root radii (R_1 and R_2) significantly affected the stress concentration of the implant threads.

Bone stresses

In this study, 14 points on the implant-bone interface were selected to find the most stressed site of the surrounding bone (Fig. 6). Among all implant models, the most stressed sites consistently occurred at the first thread. For the conical implant with the 0.6-mm pitch, the maximum stresses at the first thread were 115.2 MPa, 68.5 MPa, and 83.3 MPa for the symmetrical, square, and buttressed threads, respectively. For the symmetrical, square, and buttressed threads with the 0.6-mm pitch and a cylindrical thread taper, the maximum stresses at the first thread were 116.0 MPa, 64.5 MPa, and 82.6 MPa, respectively. The stress of the symmetrical thread was 79.8% and 40.4% higher than those of the square and buttressed threads (Fig. 7). For the symmetrical, square, and buttressed threads with the 0.8-mm pitch, the maximum stresses at the first thread were 136.0 MPa, 92.6 MPa, and 97.8 MPa, respectively. The stress of the symmetrical thread was 46.9% and 39.1% higher than those of the square and buttressed threads (Fig. 7).

Within the area (=0.156 mm^2) enclosed by the tip of the first thread, percentages of node numbers for the six ranges of nodal stress are shown in Fig. 8. For the symmetrical, square, and buttressed threads with a cylindrical taper and 0.6-mm pitch, only 9.9%, 1.0%, and 5.0% of the nodes, respectively, had stress values exceeding 60 MPa. In this study, the average stress value of the nodes around the first thread tip was also chosen as a comparison index (Fig. 7). For the conical taper, the average stress of the symmetrical thread was, respectively, 47.6% and 14.8% higher than those of the square and buttressed threads. For the cylindrical taper and 0.60-mm pitch, the average stress of the symmetrical thread was 55.0% and 24.0% higher than those of the square and buttressed threads, respectively. Regardless of the thread taper design, both were almost equally stressed at the first thread root (Fig. 7). For the 0.80-mm pitch, the aforementioned differences in the average stress were 35.7% and 22.6%. Regardless of the maximum or average stress, the stress value of the first thread for the symmetrical thread was higher than the other two.

Discussion

Within the immediate postoperative period, the initial stability of an inserted implant is a direct consequence of the geometric constraints imposed by the

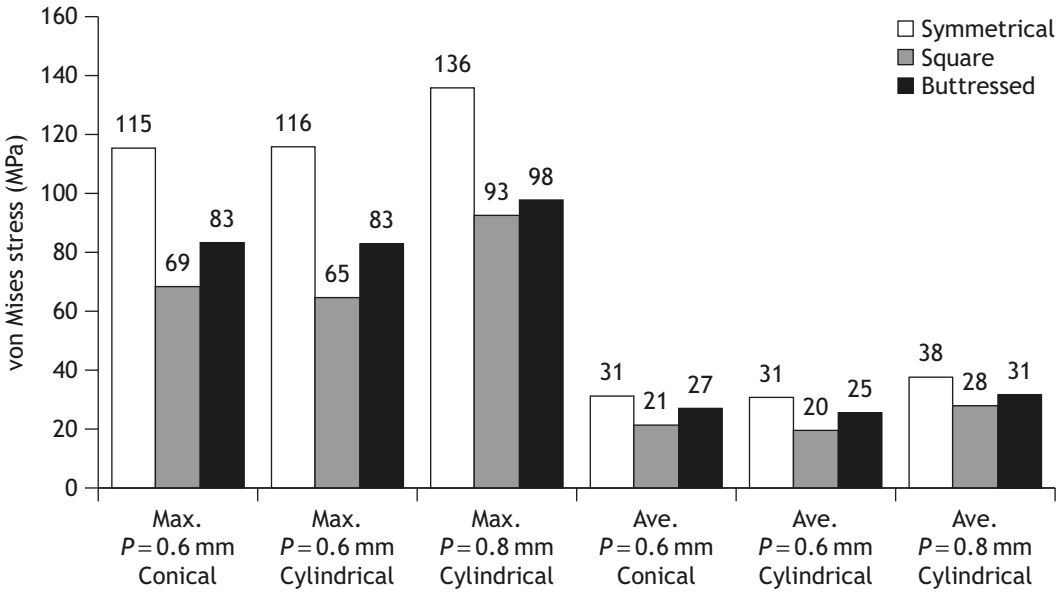

Fig. 7 Maximum and average stresses of the first mandible thread were compared among the design variations of pitch, shape, and taper. *P*=pitch.

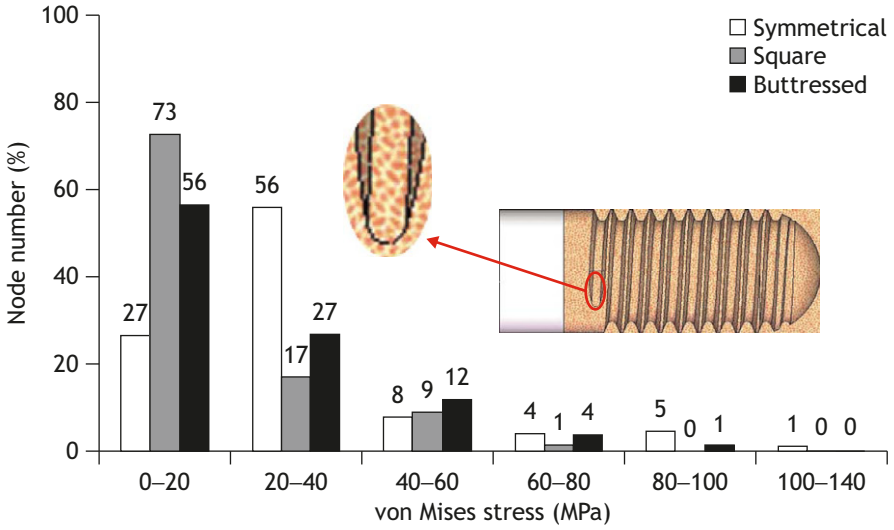

Fig. 8 For the situation of 0.60-mm pitch and tapered threads of cylindrical implants, the statistical distribution of nodal stresses within the first mandible thread is given. The area enclosing the tip of the first mandible thread was 0.156 mm^2 for the three thread shapes.

implant threads. Further stabilization of the implant is enhanced by osseointegration of the threaded surface and bone structure. In this study, we postulated that the initial stability of the implant-bone structure is closely related to the thread shape and taper of the implant. The seven parameters of thread shape and two types of thread taper were defined, and their effects on the contact area and stress distribution of the implant-bone construct were evaluated.

Contact area

Fig. 4 shows the values of the total contact area for the nine implant-bone structures within cancellous bone. Among the three thread shapes, the contact area of the square thread was the highest, followed by the buttressed one, with that of the symmetrical one the least. This indicates that the implant with square threads possesses higher total contact area at the implant-bone interface compared to the other two types. On average, the total contact area of the square thread was 9.7% and 4.8% higher than those of the symmetrical and buttressed types for the two types of thread pitch. This finding is of biomechanical significance for the surface treatment of implant threads. If the surface treatment is the same, the surface area of the roughened square threads can be reasonably assumed to still be the highest among the

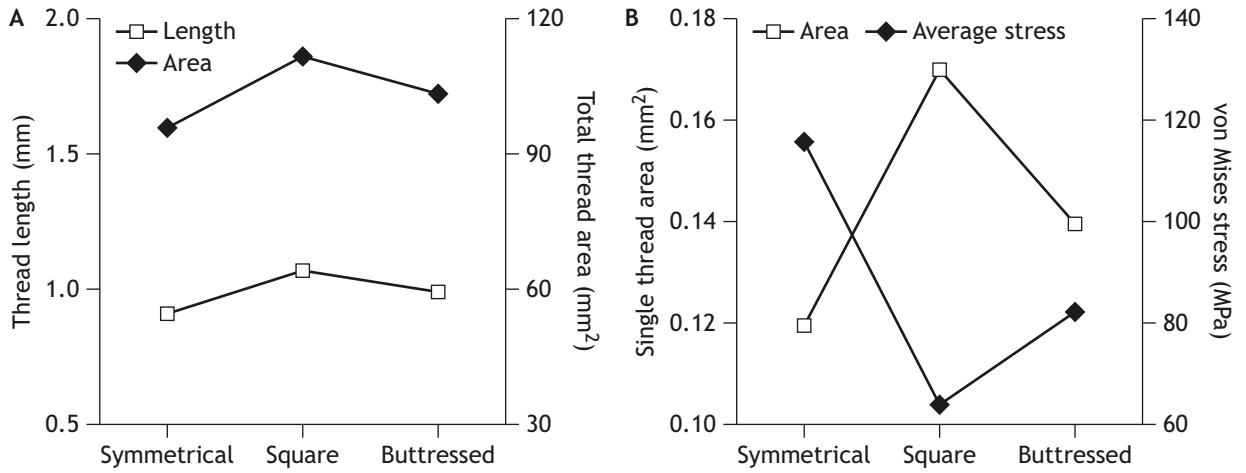

Fig. 9 For the situation of 0.60-mm pitch and tapered threads of cylindrical implants: (A) diagram shows the correlation between thread length and total thread area. Thread length was defined as the circumferential length of a single thread projected onto the sagittal plane. The total thread area was the contact area of only the threaded portion. (B) Correlation between the single thread area and the average von Mises stress of the first mandible thread.

three thread shapes. However, the thread shape might also affect insertion-induced resistance during implant surgery. In a situation of more intimate implant-bone contact, a higher torque might be necessary to overcome the insertion-induced resistance but could possibly induce heat damage to the surrounding bone. Hence, the tradeoff between the contact area and insertion resistance is important for the optimal design of the thread shape. However, these effects were not evaluated in this study, but only comparisons of the total contact area between several common thread designs were made.

After the threads of the titanium rod were lathed, the total contact area consisted of the remaining smooth and threaded surfaces below line *AB* (Figs. 3B and 5A). In this study, the widths (*W*) of the three thread shapes were identical. Thus, after lathing, the remaining areas of the smooth surface were nearly equal ($\fallingdotseq$ 35 mm^2) among the three thread shapes. For the symmetrical, square, and buttressed threads with the cylindrical taper and 0.60-mm pitch, values of the total contact area were 132 mm^2, 145 mm^2, and 138 mm^2, respectively (Fig. 4). Values of the threaded area were 96 mm^2, 111 mm^2, and 103 mm^2, respectively (Fig. 9A). Ratios of the threaded to the total contact area were 72.7%, 76.6%, and 74.6%, respectively, for the symmetrical, square, and buttressed threads. Hence, the main contributor to the total contact area was the threaded surface, at about 74.6%, rather than the remaining smooth surfaces. Apparently, the area ratio of the threaded surface for threads with the 0.80-mm pitch was less than that of the 0.60-mm pitch (Fig. 4). The reason was that the number of threads with pitch=0.60 mm (=10 threads) was more than that of pitch=0.80 mm (=7 threads) (Fig. 2B).

The contact area (=133 mm^2) for the square thread with the 0.80-mm pitch was 9.0% less than that ($\fallingdotseq$ 145 mm^2) of the square one with the 0.60-mm pitch (Fig. 4). In terms of contact areas and stress values, the thread design with the finer pitch seemed to be more ideal than the coarser one. However, in the situation of pitch=0.60 mm and *W*= 0.50 mm, the square thread had about 0.10-mm wall thickness and was prone to plastic yielding or fatigue cracking (Fig. 1). Consequently, the optimal value of the pitch for square threads was closely related to the aforementioned factors and was further investigated by experimental methods.

Figs. 5B and 5C respectively illustrate the cross-sectional area and circumferential length of a single thread projected onto the sagittal plane. For both cross-sectional area and circumferential length, the square thread possessed higher values compared to the other types. Fig. 9A shows that the contact area of only the threaded surface was highly correlated with the circumferential length of the single thread (r=0.99). For the total contact area, a very high correlation still existed (r=0.99). Thus, the circumferential length of a single thread can be used as an evaluation index for the contact area of the threaded or even the total surface.

Bone stresses

No mechanical fixation was assumed within the implant-cortex contact region in this study (Fig. 3A). Fig. 6 shows that the most stressed site for all implant models consistently occurred at the first thread of the cancellous bone rather than within the cortex region. In general, the bone stress rapidly decreased towards both the tip and head of the

implant. This finding indicates a geometric discontinuity of the implant thread, not a difference in the mechanical strength of the surrounding bone, which accounts for the stress concentration on the implanted mandible. In practice, some commercially available implants have fine threads within the cortical region for more secure and immediate fixation. However, the current study provides no further insights into whether cortical fixation will benefit from decreasing the concentrated stress at the first thread compared to cancellous fixation, as assumed in this study.

The implant threads in Fig. 5B were used to illustrate the mechanism for discussing comparisons among stress values of different thread designs. The implanted bone block was extruded and reshaped as the thread-like profile around the insertion hole (Fig. 5B). We postulate that the bone threads formed by the inserted implant play a significant role in the bone strength and stress. Fig. 5B shows the bone threads with the three types of implant thread. Among them, the structure of the square thread was the strongest, followed by the buttressed one, and then the symmetrical one which had the smallest cross-sectional area. The bone stress at the first thread also revealed similar patterns for the three implant threads (Figs. 6 and 7). However, Fig. 9B shows a negative correlation ($r = -0.96$) between the thread area of a single thread and the most concentrated stress of the first thread. Clarification of this contradiction should take the stress concentration of the root radius into consideration. Fig. 5C illustrates that stress-concentrated sites of the finite-element analyses were consistently at the root radii for all three threads. Consequently, if the root radii are well-controlled by design and/or fabrication, the probability of fatigue cracking at those sites can be reasonably assumed to be suppressed. In this study, all root radii of the three thread shapes were 0.15 mm, thus equalizing the stress-concentrating effects. Only the flank angles (θ_1 and θ_2) of the thread shape influenced the concentrated stresses. In such a situation, the square thread is a comparatively more optimal design in terms of contact area and concentrated stress.

In the literature, one of the reported advantages of the conical over the cylindrical implant includes the higher insertion torque. The higher insertion torque was inferred to result in greater initial stability. The detailed mechanism explaining such an effect has not yet been discussed. At the first mandible thread, Fig. 7 shows that the stress value of the conical design was comparable to that of the cylindrical one.

During the finite-element analysis, the current study further investigated the stress distribution of the nodes around the first thread and averaged all nodal stresses (Fig. 8). Within the area enclosed by the first thread tip, the average value of all nodal stresses showed a similar trend to the maximum value (Fig. 7). Regardless of whether the average or maximal stress was chosen as the comparison index, the symmetrical thread was the most stressed compared to the other two. This indicates that thread design significantly affects the stress of the threads themselves.

In conclusion, among the three thread shapes, the contact area of the symmetrical thread was the least, and its first thread was subjected to the greatest stresses. If the wall thickness of the square thread was kept structurally reasonable, the square thread possessed a higher contact area and lower stress value than the buttressed one. However, further evaluations of the insertion torque, holding power, and fatigue properties should be made to provide complete information about the optimal design of implant threads.

References

1. Henry PJ. Tooth loss and implant replacement. *Aust Dent J* 2000;45:150–72.
2. Hebel K, Gajjar R, Hofstede T. Single-tooth replacement: bridge vs. implant-supported restoration. *J Can Dent Assoc* 2000;66:435–8.
3. Andersson L, Emami-Kristiansen Z, Högstrom J. Single tooth implant treatment in the anterior region of the maxilla for treatment of tooth loss after trauma: a retrospective clinical and interview study. *Dent Traumatol* 2003;19(Suppl 3): S126–31.
4. Gibbard LL, Zarb G. A 5-year prospective study of implant-supported single-tooth replacements. *J Can Dent Assoc* 2002;68:110–6.
5. Engquist B, Bergendal T, Kallus T, Linden U. A retrospective multicenter evaluation of osseointegrated implants supporting overdentures. *Int J Oral Maxillofac Implants* 1988;3: 129–34.
6. Yang GL, He FM, Yang XF, Wang XX, Zhao SF. Bone responses to titanium implants surface-roughened by sandblasted and double etched treatments in a rabbit model. *Oral Surg Oral Med Oral Pathol Oral Radiol Endod* 2008;2:1–9.
7. Huang LH, Shotwell JL, Wang HL. Dental implants for orthodontic anchorage. *Am J Orthod Dentofacial Orthop* 2005;127:713–22.
8. Le Guehennec L, Soueidan A, Layrolle P, Amouriq Y. Surface treatments of titanium dental implants for rapid osseointegration. *Dent Mater* 2007;23:844–54.
9. Ivanoff CJ, Sennerby J, Johansson C, Rangert B, Lekholm U. Influence of implant diameter on integration of screw implants. An experimental study in rabbits. *Int J Oral Maxxillofac Surg* 1997;26:141–8.
10. Akkocaoglu M, Uysal S, Tekdemir I, Akca K, Cehreli MC. Implant design and intraosseous stability of immediately placed implants: a human cadaver study. *Clin Oral Implants Res* 2004;16:202–9.
11. Vidyasagar L, Apse P. Dental implant design and biological effects on bone-implant interface. *Baltic Dent Maxillofac J* 2004;6:51–4.

12. Chun HJ, Cheong SY, Han JH, et al. Evaluation of design parameters of osseointegrated dental implants using finite element analysis. *J Oral Rehabil* 2002;29:565–74.
13. Ivanoff CJ, Gröndahl K, Sennerby L, Bergström C, Lekholm U. Influence of variations in implant diameters: a 3- to 5-years retrospective clinical report. *Int J Oral Maxillofac Implants* 1999;14:173–80.
14. Abshire BB, McLain RF, Valdevit A, Kambic HE. Characteristics of pullout failure in conical and cylindrical pedicle screws after full insertion and back-out. *Spine J* 2001;1:408–14.
15. Chapman JR, Harrington RM, Lee KM, Anderson PA, Tencer AF, Kowalski D. Factors affecting the pullout strength of cancellous bone screws. *J Biomech Eng* 1996;118(Suppl 3): S391–8.
16. Merk BR, Stern SH, Cordes S, Lautenschlager EP. A fatigue life analysis of small fragment screws. *J Orthop Trauma* 2001; 15(Suppl 7):S494–9.
17. Chao CK, Hsu CC, Wang JL, Lin J. Increasing bending strength and pullout strength in conical pedicle screws: biomechanical tests and finite element analyses. *J Spinal Disord Tech* 2008;21(Suppl 2):S130–8.
18. Hansson S, Werke M. The implant thread as a retention element in cortical bone: the effect of thread size and thread profile: a finite element study. *J Biomech* 2003;36:1247–58.
19. Gallas MM, Abeleira MT, Fernandez JR, Burguera M. Three-dimensional numerical simulation of dental implants as orthodontic anchorage. *Eur J Orthod* 2005;27:12–6.
20. Akca K, Cehreli MC. Biomechanical consequences of progressive marginal bone loss around oral implants: a finite element stress analysis. *Med Bio Eng Comput* 2006;44:527–35.
21. Kayabasi O, Yuzbasioglu E, Erzincanli F. Static, dynamic and fatigue behaviors of dental implant using finite element method. *Adv Eng Software* 2006;37:649–58.
22. Holmes DC, Loftus JT. Influence of bone quality on stress distribution for endosseous implants. *J Oral Implantol* 1997; 23(Suppl 3):S104–11.
23. Rho JY, Ashman RB, Turner CH. Young's modulus of trabecular and cortical bone material: ultrasonic and microtensile measurements. *J Biomech* 1993;26:111–9.
24. Yang J, Xiang HJ. A three-dimensional finite element study on the biomechanical behavior of an FGBM dental implant in surrounding bone. *J Biomech* 2007;40:2377–85.